VĚDECKÉ SPISY VYSOKÉHO UČENÍ TECHNICKÉHO V BRNĚ

Edice Habilitační a inaugurační spisy, sv. 496
ISSN 1213-418X

Andrea Straková Fedorková

NEW COMPOSITE CATHODES FOR Li-ION BATTERIES

BRNO UNIVERSITY OF TECHNOLOGY
Faculty of Chemistry
Institute of Physical and Applied Chemistry

RNDr. Andrea Straková Fedorková, Ph.D.

NEW COMPOSITE CATHODES FOR Li-ION BATTERIES

NOVÉ KOMPOZITNÉ KATÓDY PRE Li-IÓNOVÉ BATÉRIE

Short version of Habilitation thesis
Physical Chemistry

VUTIUM

BRNO 2015

KEYWORDS

Li-ion batteries, cathodes, $LiFePO_4$, polypyrrole, sulfur, nanocomposites.

KLÍČOVÁ SLOVA

Li-iónové batérie, katódy, $LiFePO_4$, polypyrol, síra, nanokompozity.

Habilitation thesis is stored at the Faculty of Chemistry, Brno University of Technology, Purkyňova 118, 612 00 Brno.

© Andrea Straková Fedorková, 2015
ISBN 978-80-214-5133-9
ISSN 1213-418X

CONTENT

CURRICULUM VITAE

RNDr. Andrea Straková Fedorková, Ph.D.
Date of birth: 20. 06. 1984, Humenné
Nationality: Slovak
Contact: fedorkova@feec.vutbr.cz, +421 907 667 441

OBJECTIVE:

- Post-doc researcher, The Faculty of Electrical Engineering and Communication Brno University of Technology, Czech Republic
- Assistant Professor, Department of Physical Chemistry, Pavol Jozef Safarik University in Kosice, Slovakia
- Deputy Director of the Institute of Chemistry for Development and External Relations, UPJS Kosice

EDUCATION AND CAREER:

2010 – 2011 Researcher, Comenius University, Bratislava

2010PhD. Analytical chemistry, Comenius University, Faculty of Natural Sciences, Bratislava, Dissertation: Analytical characterization of polypyrrole-$LiFePO_4$ powder as positive electrode material for lithium-ion batteries.

2006M.Sc. Physical chemistry, University of Pavol Jozef Safarik, Faculty of Natural Sciences, Košice, Master degree obtained in 4 years with distinction. Diploma thesis: Preparation and characterization of porous materials with cellular structure.

2002 Secondary chemical school in Humenné

RESEARCH SKILLS, GRANTS AND FELLOWSHIPS:

April-May 2014 Research stay at Centre d'Investigació en Nanociència i Nanotecnologia, Barcelona, Spain, Prof. Pedro Gomez-Romero

November 2013 Research stay at INIFTA – Research Institute of Theoretical and Applied Physical Chemistry, Universidad Nacional de La Plata, Argentina

May-June 2013 Research stay at Centre d'Investigació en Nanociència i Nanotecnologia, Barcelona, Spain, Prof. Pedro Gomez-Romero.

October 2009 – Research stay at Technical University Wien (project APVV SK-AT-0013-08).

September-October 2008 National scholarship programme of Slovak republic, research stay at Centre d'Investigació en Nanociència i Nanotecnologia, Barcelona, Spain, Prof. Pedro Gomez-Romero.

October 2006, April-May 2007, October 2007, May-July 2008 - DAAD scholarship, research stay at Westfälische Wilhelms University, Münster, Germany, prof. Wiemhöfer – Department of Inorganic and Analytical Chemistry.

April – Jun 2005 - Socrates Erasmus scholarship, Westfälische Wilhelms University, Münster, Germany.

ECDL certificate (European Computer Driving License) (2006)

Member of Slovak Chemical Society

Member of American Nano Society

Project leader – two projects VVGS (2013-2014 and 2014-2015) for young scientists, Pavol Jozef Safarik University in Kosice, Slovakia

Co-investigator – 11 national and international projects (Slovakia, Czech Republic, EU)

LANGUAGE SKILLS:

English – fluently
German – fluently

AWARDS AND HONORS:

December 2010 – Absolute winner of the Award of the President of Slovak Republic Ivan Gasparovic Students´ personality of Slovakia 2010 – The best student in Slovak Reupublic.

Junior Chamber International Slovakia (JCIS) Award - 1st place in the field of Natural Sciences and Chemistry 2010.

Nominated for the Award of the president of Slovak Republik – Ivan Gašparovič: Students´ personality of Slovakia by dean of Comenius University Bratislava, Faculty of Natural Sciences.

June 2009 – The winner of First interactive conference of young scientists in section Analytical chemistry.

June 2006 – Graduation with Honors – scholarship of Pavol Jozef Safarik University in Kosice for excellent study results.

PUBLICATIONS AND CONFERENCES:

17 scientific publications in peer-reviewed journals with impact factor between 0,9 and 4,9. 75 SCI citations. International conferences: 9oral presentations, 4 poster presentations. More than 50 full research papers in slovak or english language.

LIST OF PAPERS INCLUDED IN HABILITATION THESIS

1. **FEDORKOVÁ Andrea**, WIEMHÖFER Hans-Dieter, ORIŇÁKOVÁ Renáta, ORIŇÁK Andrej, KANIANSKY Dušan, Surface modification of $FePO_4$ particles with conductive layer of polypyrrole, Solid State Sciences, 12 (2010) 924-928, IF = 1,907

2. **FEDORKOVÁ Andrea**, ORIŇÁKOVÁ Renáta, ORIŇÁK Andrej, TALIAN Ivan, HEILE Andreas, WIEMHÖFER Hans-Dieter, KANIANSKY Dušan, ARLINGHAUS Heinrich Frank, PPy doped PEG conducting polymer films synthesized on $LiFePO_4$ particles, Journal of Power Sources, 195, (2010) s. 3907-3912, IF = 4,951

3. **FEDORKOVÁ Andrea**, ALEJOS Ana Nacher, GÓMEZ-ROMERO Pedro, ORIŇÁKOVÁ Renáta, KANIANSKY Dušan, Structural and electrochemical studies of PPy/PEG-$LiFePO_4$ cathode material for Li-ion batteries, Electrochimica Acta, 55 (2010), s. 943-947, IF = 3,832

4. **FEDORKOVÁ Andrea**, ORIŇÁKOVÁ Renáta, ORIŇÁK Andrej, KUPKOVÁ Miriam, WIEMHÖFER Hans-Dieter, AUDINOT Jean Nicolas, GUILLOT Jerôme, Electrochemical and XPS study of $LiFePO_4$ cathode nanocomposite with PPy/PEG conductive network, Solid State Sciences, 14 (2012) 1238-1243, IF = 1,907

5. **FEDORKOVÁ Andrea**, WIEMHÖFER Hans-Dieter, ORIŇÁKOVÁ Renáta, ORIŇÁK Andrej, STAN Marian Cristian, WINTER Martin, KANIANSKY Dušan, ALEJOS Ana Nacher, Improved lithium exchange at $LiFePO_4$ cathode particles by coating with composite polypyrrole-polyethylene glycol layers, Journal of Solid State Electrochemistry, 13, (2009) 1867-1872, IF = 2,131

6. **FEDORKOVÁ Andrea**, ORIŇÁKOVÁ Renáta, ORIŇÁK Andrej, HEILE Andreas, WIEMHÖFER Hans-Dieter, ARLINGHAUS Heinrich Frank, Electrochemical and TOF-SIMS investigations of PPy/PEG-modified $LiFePO_4$ composite electrodes for Li-ion batteries, Solid State Sciences, 13 (2011) 824-830, IF = 1,907

7. **FEDORKOVÁ Andrea**, ORIŇÁKOVÁ Renáta, ORIŇÁK Andrej, WIEMHÖFER Hans-Dieter, AUDINOT Jean Nicolas, GUILLOT Jerôme, $LiFePO_4$ cathode nanocomposite with PPy/PEG conductive network, ECS Transactions,40 (1) (2012) 107 – 115

8. FILKUSOVÁ Mária, **FEDORKOVÁ Andrea**, ORIŇÁKOVÁ Renáta, ORIŇÁK Andrej, NOVÁKOVÁ Zuzana, ŠKANTÁROVÁ Lenka, Effect of multi-walled carbon nanotubes on the thermal stability and surface morphology of $LiFePO_4$ cathode material, New Carbon Materials, 28 (2013) 1-7, IF = 0,981

9. **FEDORKOVÁ Andrea**, ORIŇÁKOVÁ Renáta, ORIŇÁK Andrej, WIEMHÖFER Hans-Dieter, KANIANSKY Dušan, WINTER Martin, Surface treatment of $LiFePO_4$ cathode material with PPy/PEG conductive layer, Journal of Solid State Electrochemistry, 14 (2010) 2173-2178, IF = 2,279

10. ČECH Ondřej, THOMAS Jorge E., SEDLARIKOVÁ Marie, **FEDORKOVÁ Andrea**, VONDRÁK Jiří, MORENO Mario Sergio, VISINTIN Arnaldo, Performance improvement on $LiFePO_4$/C composite cathode for lithium-ion batteries, Solid State Sciences, 20 (2013) 110-114, IF=1,907

11. **FEDORKOVÁ Andrea**, ORIŇÁKOVÁ Renáta, ČECH Ondrej, SEDLAŘÍKOVÁ Marie, New composite cathode materials for Li/S batteries: A review, Int. J. Electrochem. Sci., 8 (2013) 10308-10319, IF = 3,729

12. ORIŇÁKOVÁ Renáta, **FEDORKOVÁ Andrea**, ORIŇÁK Andrej, Effect of PPy/PEG conducting polymer film on electrochemical performance of $LiFePO_4$ cathode material for Li-ion batteries – Review, Chemical Papers, 67 (2013) 860-875, IF = 0,879

1 INTRODUCTION

Today, the modern world cannot be described without considering lithium-ion batteries. Current concern about limited energy resources, coupled to the need to decrease greenhouse gas emissions, has brought the need to consider renewable energies at a large scale together with the use of hybrid and electric vehicles. Among the various energy conversion/storage systems proposed over the two last centuries, electrochemical storage and more specifically batteries seem to be very well positioned to satisfy these needs, but research to meet the application requirements is still an imperious need [1].

Current lithium-ion battery technology consists of $LiCoO_2$ and graphite, which is the first generation of lithium-ion batteries. The lithium-ion batteries currently available in market range in capacity from 550 mAh to 2.5 Ah for portable applications and up to 45 Ah for motive power and stationary applications. In order to advance lithium-ion batteries, several concepts have been developed, leading to innovative new positive and negative electrode materials.

Lithium-ion batteries were first commercialized in 1990 [2] as a natural result of the extensive knowledge in intercalation chemistry accumulated by inorganic and solid state chemists in the 1970s [3,4]. The first generation of such batteries allowed storing more than twice the energy compared to nickel or lead batteries of the same size and mass. It consisted of $LiCoO_2$ and carbon at the positive and negative electrode, respectively, the redox operation of both versus lithium being based on intercalation reactions. However, both existing and new emerging applications demand even better performance in terms of energy density, power, safety, price and environmental impact [5]. As a consequence, mature as the technology may seem at first sight, the quest for improved materials had never been so intense. In these almost 20 years of life of the lithium-ion battery, we have witnessed continuous progress in intercalation materials, [6,7] and alternatives to $LiCoO_2$, such as $LiNi_{1-y-z}Mn_yCo_zO_2$, $LiFePO_4$ and $Li_4Ti_5O_{12}$, have reached the market at different levels, bringing about incremental improvements in performance. All these materials have intrinsic limitations in terms of capacity, which are derived from their redox mechanism of operation and structural aspects. Indeed, the reversible intercalation of lithium ions is mostly limited by the changes the crystal structure and to the intrinsic limited redox activity (i.e., number of exchanged electrons) of the transition metals.

Therefore, changing the battery chemistry from current lithium intercalation reactions in transition metal oxides or metal phosphates or graphite to other promising reactions is an inevitable means to boost the performance of Li-ion batteries.

Lithium-sulfur (Li-S) batteries are regarded as one of the next-generation energy storage systems due to the extremely low-cost sulfur and their high energy density [8-10]. The price of sulfur per metric ton was as low as \$160 USD in 2012 [11]. The theoretical capacity of sulfur is 1672 mAh/g (calculated based on $S^0 \leftrightarrow S^{2-}$). Coupled with the average operating voltage of a Li-S cell (2.15 V vs Li^+/Li^0) and the theoretical capacity of a pure lithium anode (3862 mAh/g, calculated based on $Li^+ \leftrightarrow Li^0$), the energy density can be estimated as high as ~2500 Wh/kg, which is an order of magnitude higher than that of traditional Li-ion batteries.

Battery technology has come a long way since the Italian physicist Alessandro Volta in 1800 described the first electrochemical cell, which came to be known as the Volta pile [12]. Today, research in the battery world is focused on the Li-ion battery, which has a great advantage over other battery concepts (Fig. 1) [13]. G.N. Lewis initiated the first work on lithium-based batteries already in 1912, but it was not until the early 1970s that the first commercial primary lithium battery reached the market [14]. In these early batteries, TiS_2 was used as active cathode material, lithium foil as anode and lithium perchlorate in dioxolane as electrolyte [15].During discharge, the Li^+ ions from the metallic lithium anode are inserted into the empty octahedral sites of the layered TiS_2 cathode, which is accompanied by a reduction of the Ti^{4+} ions into Ti^{3+} ions. During charge, exactly the reverse reaction occurs. The layered structure of TiS_2 is maintained during the charge-discharge (lithium extraction/insertion) process, resulting in good reversibility. Following this, several other sulfides and chalcogenides with high capacities were investigated during the 1970s and 1980s as cathodes [16]. However, most of them exhibited a low cell voltage of < 2.5 V versus a metallic lithium anode. This limitation in cell voltage is due to the overlap of the higher valent Mn^{+}:d band with the top of the nonmetal:p band. For example the overlap of the Co^{3+}:3d band with the top of the S^{2-}:3p band in cobalt sulfide results in an introduction of holes or removal of electrons from the S^{2-}:3p band and the formation of molecular ions such as S_2^{2-}. This results in an inaccessibility of the higher oxidation states of the Mn^{+}ions in a sulfide like M_yS_z, leading to a limitation in cell voltage to < 2.5 V. Recognizing this difficulty with chalcogenides, Goodenough’s group at the University of Oxford focused on oxide cathodes during the 1980s [17-19]. The larger Madelung energy in an oxide compared to that in a sulfide as well as the lying of the top of the O^{2-}:2p band below that of the S^{2-}:3p band make the higher valence states accessible in oxides. For example, while Co^{3+} can be readily stabilized in an oxide, it is difficult to stabilize Co^{3+} in a sulfide since the $Co^{2+/3+}$ redox couple lies within the S^{2-}:3p band. Accordingly, several transition metal oxide hosts (*e.g.*, $LiCoO_2$ and$LiMn_2O_4$) providing ~ 4 V vs. Li/Li^{+} were identified as lithium intercalation cathodes during the past three decades. Although the cell voltage could be raised significantly with the oxide cathodes, rechargeable lithium cells based on metallic lithium anode could not be commercialized because of the safety problems associated with metallic lithium [20,21].The inherent safety problem of metallic lithium anode and the dendrite formation during the charge-discharge cycling eventually forced the use of intercalation compounds as anodes. This led to the commercialization of the lithium-ion battery technology by Sony in 1990 with $LiCoO_2$ as the cathode and graphite as the anode.

The earliest configuration of a Li–S battery was presented in the late 1960s [22,23]. The positive electrode comprised elemental sulfur, electronic conductors (carbon or metal powder) and binders, separated from the metallic lithium negative electrode by an organic electrolyte. This configuration has been the platform for subsequent major research activities as well.

2 CATHODE MATERIALS

In this chapter the most suitable materials used for Li-ion and Li-S rechargeable batteries are discussed.

2.1 INTERCALATION VS. CONVERSION

Intercalation is when molecule X is inserted/intercalated between the graphite layers (anode). In this type of compound, the graphite layers remain largely intact and the guest molecules or atoms (Li^+) are located in between. When Li-ion cell is discharging, the lithium is extracted from the anode and inserted into the cathode. When the cell is charging, lithium is extracted from the cathode and inserted back into the anode (Fig. 1).

Conversion is based on reaction of lithium and sulphur to lithium sulfide:

$$16Li + S_8 \rightarrow 8Li_2S \tag{1}$$

The electrodes in this cell (Fig. 2) mainly consist of metallic lithium (negative electrode, anode during discharging) and sulfur (positive electrode, cathode during discharging). During discharge lithium is oxidized, the Li^+ ions are dissolved in the solvent and move towards the cathode. There, they react with reduced sulfur to finally produce Li_2S via several intermediates (the polysulfides).

$S_8 \rightarrow Li_2S_8 \rightarrow Li_2S_6 \rightarrow Li_2S_4 \rightarrow Li_2S_3 \rightarrow Li_2S_2 \rightarrow Li_2S$

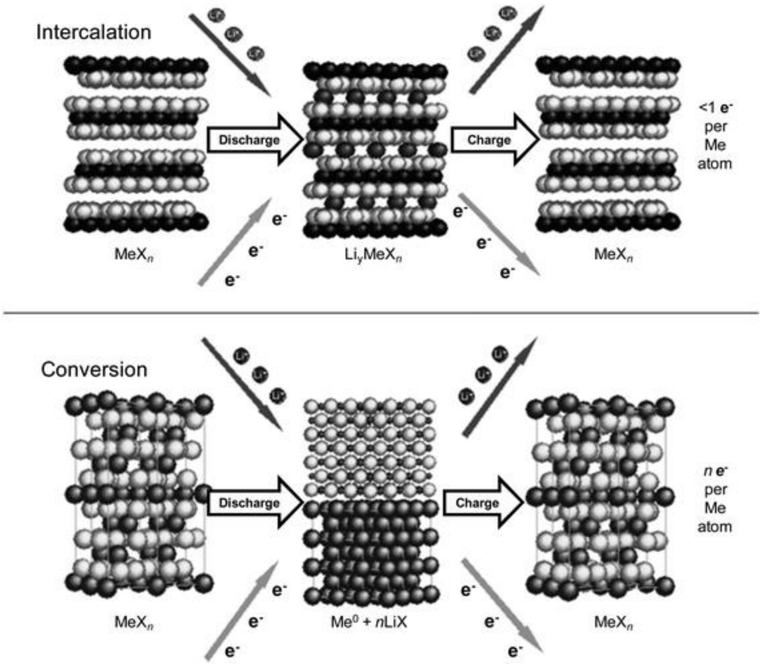

Figure 1. Difference between intercalation and conversion in lithium battery [24].

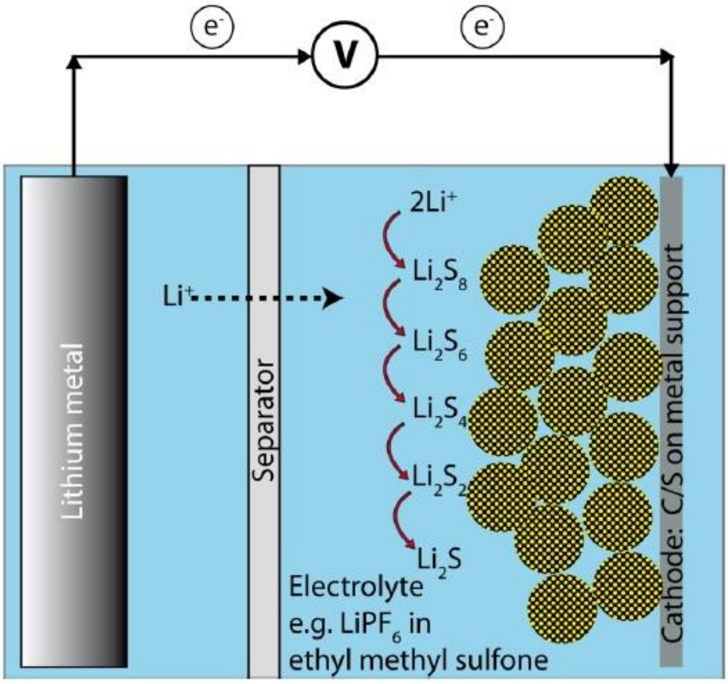

Figure 2. Schematic representation of Li-S battery [25].

2.2 CATHODE MATERIALS FOR LITHIUM BATTERIES

The increasing demand for batteries has led vendors and academics to focus on improving the energy density, operating temperature, safety, durability, charging time, output power, and cost. One of the possible solutions is to find new nanostructured composite cathode materials or improve the properties of existing materials.

Table 1. Comparison of some properties for various cathode materials [26].

Cathode Material	Average Voltage [V]	Gravimetric Capacity [mAh/g]	Gravimetric Energy [kWh/kg]
$LiCoO_2$	3.7	140	0.518
$LiMn_2O_4$	4.0	100	0.400
Li_2S	2.3	1672 mAh/g_{sulfur}	2.567
$LiNiO_2$	3.5	180	0.630
$LiFePO_4$	3.3	150	0.495

Li_2FePO_4F	3.6	115	0.414
$LiCo_{1/3}Ni_{1/3}Mn_{1/3}O_2$	3.6	160	0.576
$Li(Li_aNi_xMn_yCo_z)O_2$	4.2	220	0.920

2.2.1 **$LiCoO_2$**

$LiCoO_2$ (Fig. 3) is the most commonly used cathode material in commercial Li-ion batteries today by virtue of its high working voltage, structural stability and long cycle life [27]. The electrode potential for fully delithiated $LiCoO_2$ is very attractive (4.7 V *vs.* Li°/Li^{+}) and would result in a very high gravimetric energy density for the full lithium extraction. However, at these high voltages, irreversible structural changes occur caused mainly by exothermic reactions with the electrolyte [28,29]. Because of this, only half of the available lithium is allowed to be extracted from $LiCoO_2$ in commercial batteries. This means that the voltage never exceeds 4.2 V *vs.* Li°/Li^{+} and that the theoretical capacity is limited to 130 mAhg^{-1}. However, Co is an expensive metal and much effort has been made in recent years to find a cheaper alternative. $LiNiO_2$ (isostructural with $LiCoO_2$) and spinel type $LiMn_2O_4$ are promising materials in this respect, with $LiNiO_2$ the more attractive alternative because of its high specific capacity and better elevated-temperature performance.

2.2.2 **$LiFePO_4$**

In 1997, Padhi *et al.* described a new class of intercalation compounds that had the composition $LiMPO_4$ (M=Fe, Mn, Co, Ni) [30]. These were termed phospho-olivines because of their resemblance to the mineral olivine, $(Mg,Fe)_2SiO_4$. $LiFePO_4$ (Fig. 3) was soon recognised as the most promising candidate in this group [31]. $LiFePO_4$ exhibits several attractive attributes; it is environmentally benign, cheap to produce, and thermally and mechanically stable. It also has a very flat voltage plateau at 3.45 V *vs.* Li°/Li^{+}, which, is easy to work with and has a high theoretical capacity of 170mAh/g, based on the extraction of all lithium. The introduction of $LiFePO_4$ into commercial batteries was, however, for a long time hindered by its one major drawback: its poor electronic conductivity. A lot of research has been devoted to this one problem, which has resulted in several ways to combat it. Coating$LiFePO_4$ particles with a highly conductive agent such as carbon [32-34], decreasing the actual size of the $LiFePO_4$ particles [35-37], and cycling the batteries with $LiFePO_4$ cathodes at a higher temperature than room temperature [38] are all partial solutions to this problem of low electronic conductivity.

2.2.3 **$LiMn_2O_4$**

$LiMn_2O_4$ (Fig. 3) spinel phase is one of the most promising cathode materials for lithium ion rechargeable batteries because it offers many advantages such as high energy density, higher cell voltage, low cost and low toxicity over other rechargeable systems [39]. However, in bulk electrode systems, $LiMn_2O_4$ shows relatively poor performance at high charge and discharge rates and significant capacity fading during cycling, which are key requirements for applications such as battery for electric vehicles. The rate-limiting process for charging/discharging is controlled by the intercalation/de-intercalation or diffusion of Li ions into the host materials at the cathode while the capacity fade is controlled by the stability of $LiMn_2O_4$ phase over hundreds of cycles [40]. A systematic control of microstructure of these films is not only of great interest from a technological point of view but is also extremely necessary to understand the electrochemical behaviour of electrodes, which are extremely sensitive to their stoichiometry, composition, structure and morphology [41,42].

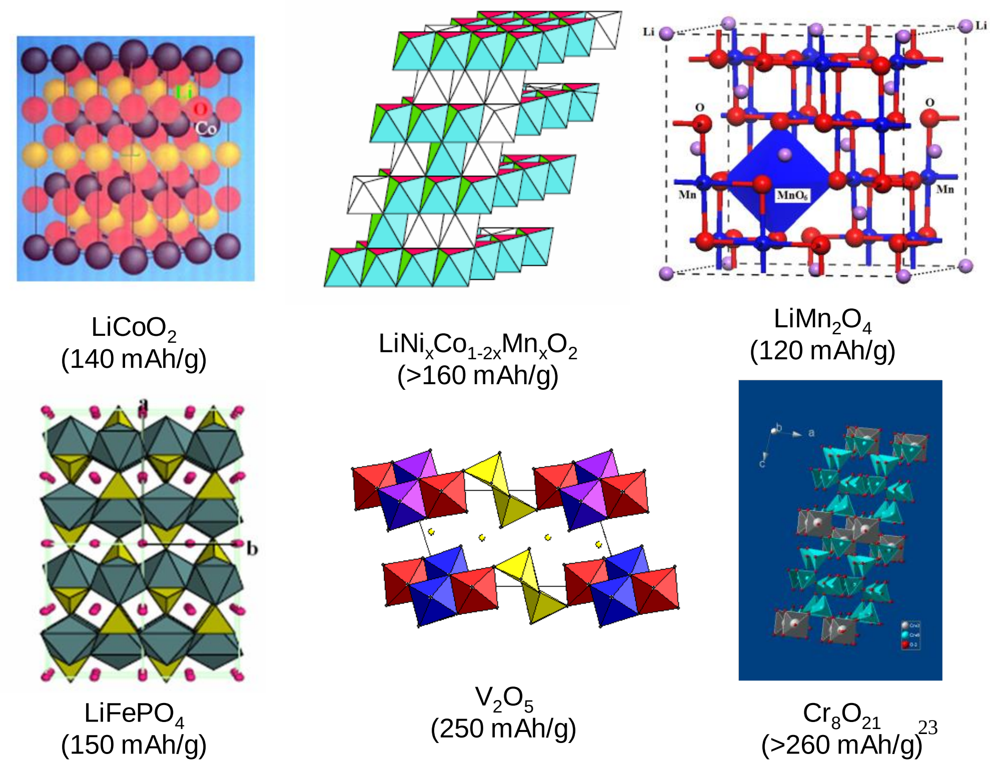

$LiCoO_2$
(140 mAh/g)

$LiNi_xCo_{1-2x}Mn_xO_2$
(>160 mAh/g)

$LiMn_2O_4$
(120 mAh/g)

$LiFePO_4$
(150 mAh/g)

V_2O_5
(250 mAh/g)

Cr_8O_{21}
(>260 mAh/g)[23]

Figure 3.The crystal structure of some cathode materials for Li-ion batteries.

2.2.4 **Sulfur**

Sulfur is a promising cathode material because of its high specific capacity and energy density [43-45]. Sulfur reacts with lithium to form lithium sulfide according to equation:

$$2Li + S \rightarrow Li_2S \qquad (2)$$

Theoretically, for every gram of sulfur in the cathode, 433 mg of lithium is required for the reaction in equation 2 to go to completion. Therefore, the theoretical gravimetric capacity of the lithium-sulfur battery with respect to the combined mass of sulfur and lithium is1167 mAh/g. With an average discharge voltage of approximately 2.2 V, the energy density of the battery is 2567 mWh/g [46]. Present day lithium-sulfur batteries consist of solid-state sulfur composite cathodes, which incorporate a conductive carbon additive and an organic polymer binder. State-of-the-art lithium sulphur batteries consist of cathodes in which sulfur is contained within an ordered nanostructured carbon framework to prevent capacity fading due to loss of active mass to the electrolyte. When the carbon is functionalized with polyethylene glycol, these cathodes exhibit reversible capacities of~1100 mAh/g (with respect to sulfur mass).

The electrochemical reduction of sulfur is very complicated, composed of a series of electron transfer reactions [46]. Yamin *et al.* have electrochemically characterized Li_2S_8 with cyclic voltammetry, using glassy carbon, stainless steel, and porous teflon-bonded carbon as the working, counter, and reference electrodes, respectively [43]. CV analysis is summarized in Fig. 4. When sweeping in the cathodic direction (i.e., towards negative potentials), three reduction (or cathodic) peaks are observed. The first cathodic peak is attributed to the reduction of higher order polysulfides (i.e., $n \geq 7$) to S_6^{2-} (point 1), while the second cathodic peak is attributed to the reduction of S_6^{2-} to S_5^{2-} (point 2). The third cathodic peak is attributed to the reduction of S_5^{2-} to both Li_2S_2 and Li_2S (point 3). However, when the potential is swept in the anodic direction (i.e., towards positive potentials), only one oxidation (or anodic) peak is observed. In the literature, this anodic peak is attributed to the simultaneous oxidation of all polysulfides to elemental sulfur (point 4).

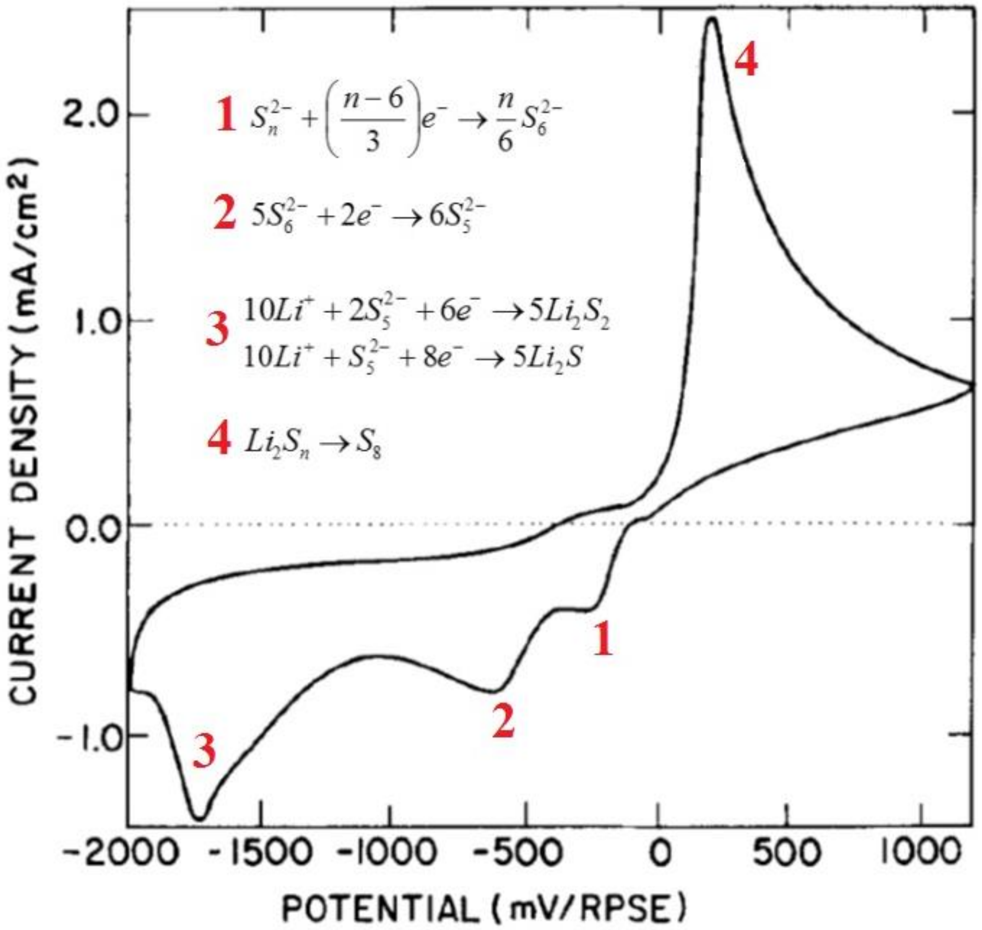

Figure 4. Cyclic voltammogram of 4 mM Li_2S_8, cathodic direction. Electrodes: glassy carbon, working; stainless steel, counter; porous teflon-bonded carbon, reference. Electrolyte: 0.8M $LiClO_4$ in THF. Sweep rate: 50 mV/s. Potential: vs. reference polysulfide electrode (RPSE) (Adapted from Yamin *et al.*) [43].

3 RESULTS AND DISCUSSION

This chapter presents the main results obtained during more than 7 year investigation focused on the new cathode material for Li-ion batteries based on $LiFePO_4$ and modified with different additives and conductive coatings. Next few chapters contain either links on selected articles in per-reviewed scientific journals with impact factor between 0.9 and 4.8. The most important articles with fundamental results and conclusions are also attached in the habilitation thesis (App1−App12).

3.1 SURFACE MORPHOLOGY OF CATHODE MATERIAL

The scanning electron microscope (SEM) image of the typical $LiFePO_4$ powder particles obtained by the solvothermal process is shown in Fig. 5a [47]. The powder material consisted of ellipsoidal particles with the diameter in the range from about 500 nm to 1μm. Some particles formed agglomerates of 1.5 – 2 μm. The particle size is smaller than the size of $LiFePO_4$ particles synthesized by solvothermal procedure with utilization of autoclave [48].

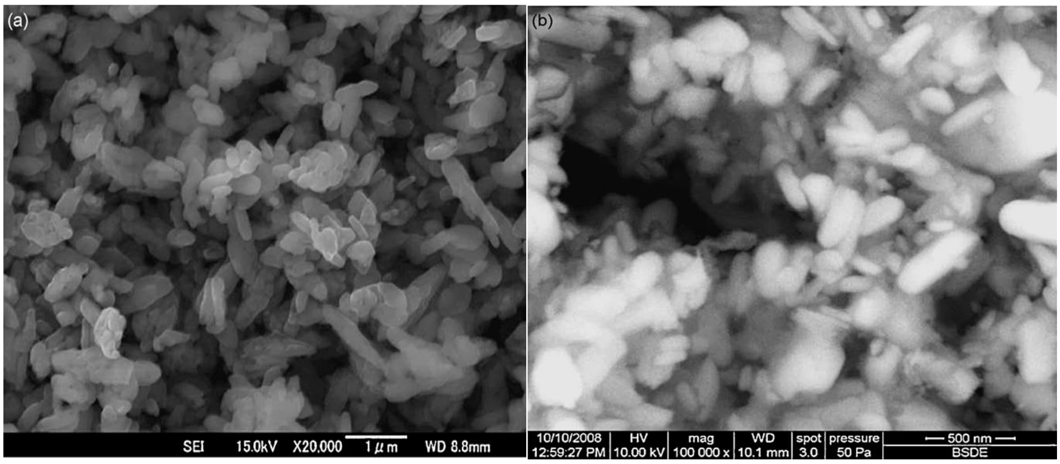

Figure 5. SEM image of pure $LiFePO_4$ (a) and $LiFePO_4$ particles covered with PPy (b).

The synthesis of powder material with an appropriate size of particle is very important to prepare an efficient battery system based on the $LiFePO_4$ cathode. The $LiFePO_4$ particles with PPy coating layer are shown in Fig. 5b. The PPy polymeric layer is continuously spread onto the whole composite material which is very important for an effective lateral electron transfer over the surface of particle in a resulting cathode material. The $LiFePO_4$ particles are coated with the ~100 nm PPy layer and some fraction of PPy is unequally dispersed among the coated particles and aggregates. Smaller particles favour the bonding of PPy with $LiFePO_4$ to advance the good electronic transport between the cathode material particles and current collector. Moreover, they provide shorter distances for diffusion of Li^+ ions in the cathode material and facilitate transfer of the electrolyte, which is beneficial to improve the electrochemical performance of $Li/LiFePO_4$ batteries [47, 49-51].

For that reason, the particle size range of prepared samples was explored in more detail. The results of particle size distribution analyses are presented in Fig. 6 . [47]. While the bare $LiFePO_4$ particles (Fig. 6a) are characterized by a very tight distribution (average diameter 1.64 μm), the PPy–$LiFePO_4$ particle size distribution (Fig. 6b) is absolutely different. Three granulometric classes were registered for the PPy–$LiFePO_4$ particles: 0.1 – 0.8, 0.8 – 8 and 8 – 20 μm (Fig. 6b). The PPy fragments originated during the chemical polymerization of Py, which take place in the bulk (not on the surface of $LiFePO_4$ particles) belong to the smallest size fraction. The uncoated $LiFePO_4$ particles, PPy coated $LiFePO_4$ particles and clusters constituted the medium granulometric class.

The aggregates of PPy, $LiFePO_4$ and PPy–$LiFePO_4$ particles formed the largest granulometric fraction. The median diameter value determined for PPy–$LiFePO_4$ sample is 4.92 μm [47].

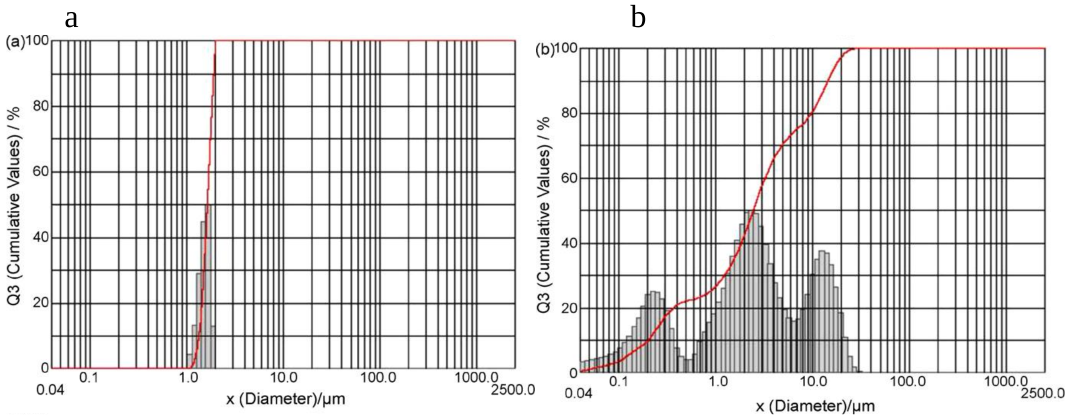

Figure 6. Particle size distribution of pure $LiFePO_4$ (a) and PPy–$LiFePO_4$ particles (b).

The conductivity and quality of the PPy layer may be enhanced by introduction of additional reagents as enzymes, molecular oxygen or PEG [52,53]. The coupling of PPy with PEG may be applied to enhance the conductivity of resulting PPy/PEG-$LiFePO_4$ electrode material without the specific capacity decrease. The electronic conduction of bare $LiFePO_4$ and PPy-$LiFePO_4$ material was at magnitude of 10^{-7} Scm^{-1} and 10^{-4} Scm^{-1}respectively. The electronic conductivity of PPy/PEG-$LiFePO_4$ increased to 10^{-3} S cm^{-1}after doping with PEG [49]. When low amount of PEG was used (up to 0.3 mmol), the stabilizing effect indicating less structural defects and reduced cross-linking was observed [54]. Any difference of the surface morphology was registered for PPy/PEG–$LiFePO_4$ samples in comparison with PPy-$LiFePO_4$ samples [47].

The improved porosity which can enhance good electrical contact between the PPy layer and $LiFePO_4$ particles is additional benefit of the PPy coating. Moreover, high porosity can support the electrolyte penetration in the cathode material and thus promote the solid-state diffusion kinetics and enhance the rate performance, electrochemical cyclability and specific capacity of the electrode [51].

By blending of active $LiFePO_4$ based powder material with polyvinylidene fluoride (PVDF) in N-methyl-2-pyrrolidon and Super P (carbon black) in a weight ratio of 80:10:10 was prepared the slurry. Figure 7 [55,56] shows the SEM images of an aluminum foil with thin layer of slurry mixture prepared by using the bare $LiFePO_4$ (a), PPy–$LiFePO_4$ (b) and PPy/PEG–$LiFePO_4$ cathode material. The SEM micrograph of PPy/PEG-$LiFePO_4$ hybrid material clearly exhibits the higher porosity as compared with the PPy-$LiFePO_4$ and non-modified $LiFePO_4$. The $LiFePO_4$ particles were covered with the PPy and PPy/PEG polymer layers with a tissue-like structure. The extensive clusters of PPy were observed in the case of PPy-$LiFePO_4$ sample (Fig. 7b). The significant change in the surface morphology was registered after addition of PEG to the PPy-$LiFePO_4$ sample. The uniform distribution of PPy/PEG clusters and pores over the active material surface was detected [55,56].

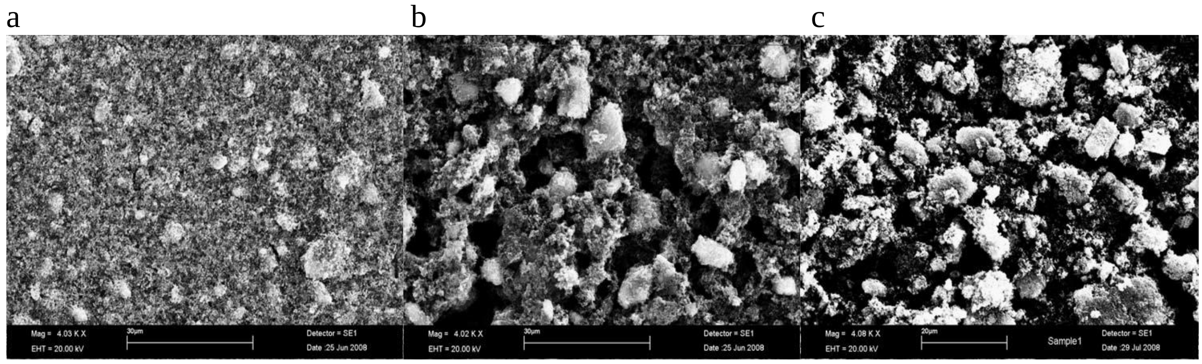

Figure 7. Aluminum foil with the thin layer of slurry prepared from pure $LiFePO_4$ (a), from PPy–$LiFePO_4$ (b) and from PPy/PEG–$LiFePO_4$ (c).

3.2 ELECTROCHEMICAL PERFORMANCE OF CATHODE MATERIAL

The effect of PPy and PPy/PEG thin layer deposition on electrochemical properties of the prepared $LiFePO_4$ based positive electrodes was evaluated by means of cyclic voltammetry, electrochemical impedance spectroscopy, and galvanostatic charge/discharge measurement. All electrochemical tests were conducted on PPy-$LiFePO_4$ and PPy/PEG-$LiFePO_4$ composites with 21% content of PPy.

Fig. 8 shows the cyclic voltammograms of cathodes prepared from $LiFePO_4$, PPy–$LiFePO_4$ and from PPy/PEG–$LiFePO_4$ [47,56]. The couple of reversible oxidation and reduction peaks was detected between 3.3 and 3.5 V vs. Li/Li^+ which correspond to the charge-discharge reaction of the Fe^{2+}/Fe^{3+} redox pair [57,58]. Only the moderate shift in potential of the anodic and cathodic peak was registered. Distances between the peak potentials for $LiFePO_4$, PPy-$LiFePO_4$ and PPy/PEG-$LiFePO_4$ cathodes are 376 mV, 186 mV and 150 mV, respectively. These results approved the notable electrode kinetics of tested cathode materials owing to improved electronic conduction arisen from the polymer coating. The PPy/PEG-$LiFePO_4$ positive electrode exhibited better reversibility and conductivity than PEG free cathodes [47,56,59].

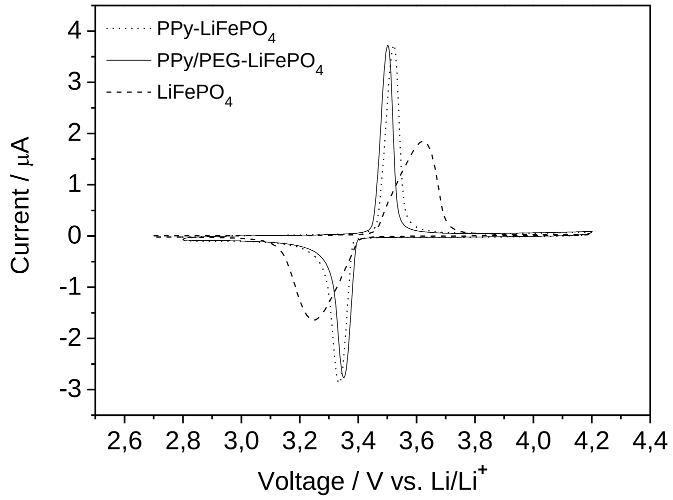

Figure 8. Cyclic voltammograms (3rd cycle) of $LiFePO_4$, PPy–$LiFePO_4$ and PPy/PEG–$LiFePO_4$ electrodes obtained at potential scan rate 50 mVs^{-1} at room temperature.

Moreover, registered CV profiles revealed a single electrochemical reaction occurred during the charge-discharge process of developed cathodes. The PPy–$LiFePO_4$ and PPy/PEG–$LiFePO_4$ electrode samples exhibited higher activity than the $LiFePO_4$ sample without polymer coating. The voltammograms reflect the electrochemical properties of both, the active material and the whole electrode. It should be noted that the reaction is diffusion of Li^+ inside the solid combined with a phase change:

$$Li^+ + e^- + FePO_4 \rightarrow LiFePO_4 \quad (3)$$

The process is more complex than a single electrode reaction limited to the electrode surface and is associated with the transport overvoltage superposition [47].

The sequence of oxidation and reduction peaks in the potential range from 3.2 V to 3.8 V associated with Fe^{2+}/Fe^{3+} redox couple at different scan rate is shown on voltammograms in Figure 9 [60]. The corresponding insertion and extraction of Li^+ ions can be observed with gradual scan rate increase from 0.2 mVs^{-1} to 5 mVs^{-1}, which indicates excellent rate performance of PPy/PEG-$LiFePO_4$ cathode material.

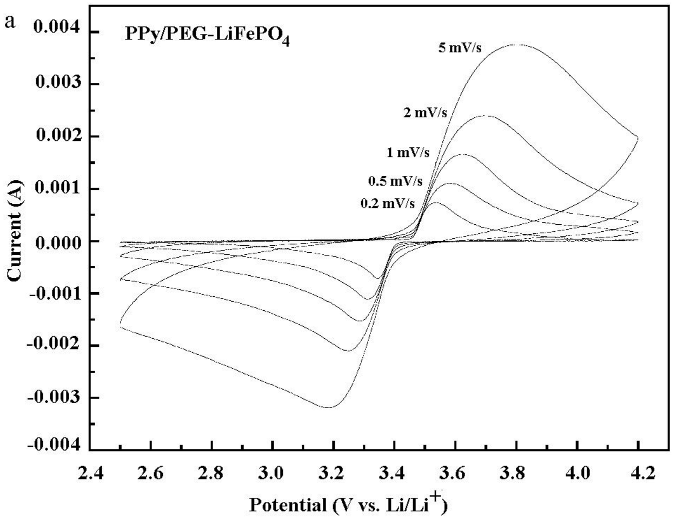

Figure 9. Cyclic voltammetry tests of the prepared PPy/PEG-$LiFePO_4$ in the potential window 2.5 – 4.2 V at different scan rates.

The galvanostatic charge-discharge profiles of bare $LiFePO_4$, PPy-$LiFePO_4$ and PPy/PEG-$LiFePO_4$ at a current rate of C/5 are displayed in Figure 10 [49]. The flat plateau for both, charging and discharging curves was registered for $LiFePO_4$ sample. The potentials of charging and discharging are about 3.49 V and 3.38 V. The initial values of charge and discharge capacity of $LiFePO_4$ at room temperature are 148 $mAhg^{-1}$and 147 $mAhg^{-1}$with a plateau at 3.5 V and 3.4 V, respectively. The discharge capacity values of 150 $mAhg^{-1}$ and 153 $mAhg^{-1}$were determined for PPy-$LiFePO_4$ and PPy/PEG-$LiFePO_4$ samples [49].

Dependence of discharge curves of all three samples ($LiFePO_4$, PPy-$LiFePO_4$ and PPy/PEG-$LiFePO_4$) on C-rates is displayed in Fig. 11 [56]. The highest specific capacity of 154 mAh $g^{-1}$was obtained on PPy/PEG-$LiFePO_4$ cathode at the lowest examined discharge rate (C/5). Both hybrid samples (PPy-$LiFePO_4$ and PPy/PEG-$LiFePO_4$) well endured high-rate charge-discharge tests, maintaining capacity values at more than half of their initial capacities when increasing rate from a C/5 to a desired 5C. Furthermore, it was observed that the sample containing PPy/PEG admixture exhibited better performance than the sample with PPy additive. The specific capacity loss of 50.3% and 40% from C/5 to 5C was registered for PPy-$LiFePO_4$ and PPy/PEG-$LiFePO_4$ cathode materials respectively.

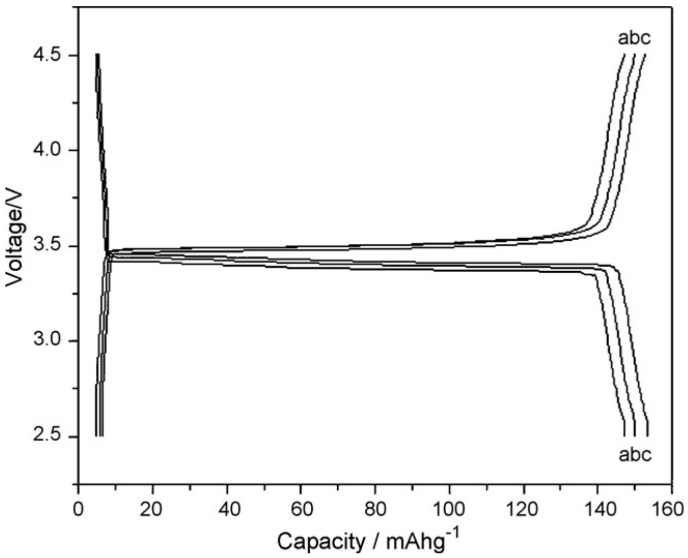

Figure 10. Initial charge and discharge curves of bare $LiFePO_4$ (a), PPy-$LiFePO_4$ (b) and PPy/PEG-$LiFePO_4$ (c) at constant rate C/5.

The observed enhanced performance of PPy/PEG-$LiFePO_4$ cathodes is more obvious at higher charge-discharge rates (2C -5C) with about 20% better specific capacity at a current rate of 5C. Addition of PEG to the $LiFePO_4$ based cathode material improved both the specific capacity and charge-discharge performance under high current rates [49,56].

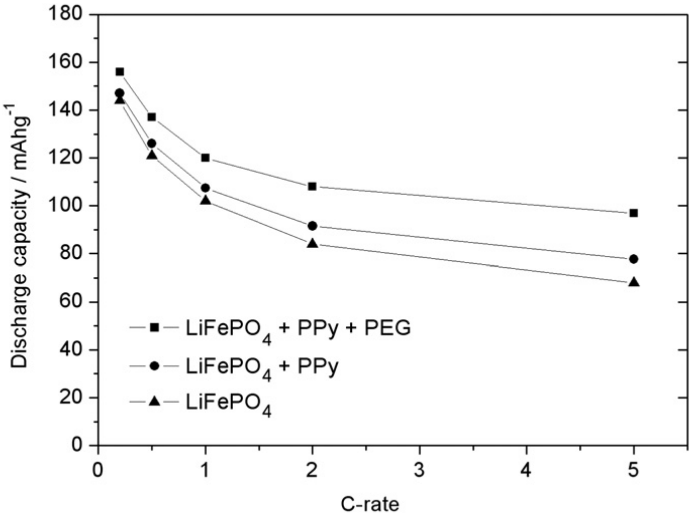

Figure 11. The first discharge curves of cathode materials made from $LiFePO_4$ (a), PPy-$LiFePO_4$ (b) and PPy/ PEG-$LiFePO_4$ (c) at variable C rates.

Figure 12 [49] shows the specific discharge capacity curves depending on number of cycles at a C/5 rate within the voltage range from 2.5 V to 4.5 V for bare $LiFePO_4$ and $LiFePO_4$ composites with PPy and PPy/PEG polymer layers.

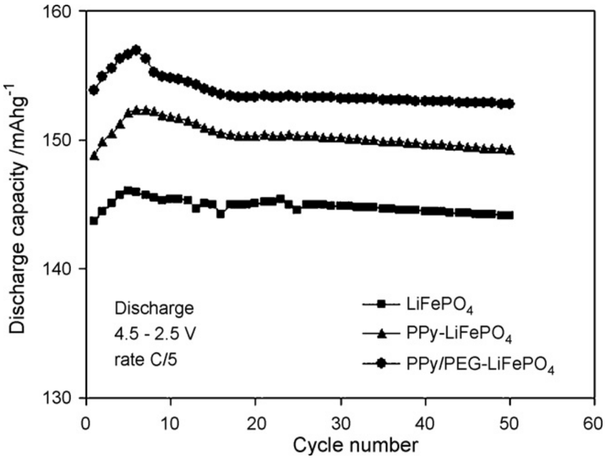

Figure 12. Dependences of discharge capacity on cycle number for LiFePO$_4$, PPy-LiFePO$_4$ and PPy/PEG-LiFePO$_4$ samples at a rate of C/5.

The specific capacity increased with increasing number of cycles during the few first (6–7) cycles and then achieved the nearly constant value indicating superior stability. Unmodified LiFePO$_4$ cathode exhibited lower cycling stability than the LiFePO$_4$ composites. These results indicated that the polymer coating layer improved the electronic conductivity of LiFePO$_4$ cathode material and facilitate the inter-grain connection in hybrid electrode [49]. The discharge capacities of LiFePO$_4$, PPy–LiFePO$_4$ and PPy/PEG–LiFePO$_4$ samples at C/5 rate were 138 mAhg^{-1}, 146 mAhg^{-1}and 148mAhg^{-1}, respectively [47]. The improved capacity of hybrid samples (PPy-LiFePO$_4$ and PPy/PEG-LiFePO$_4$) may be associated with excellent conductivity of PPy and PPy/PEG polymers. From Fig. 12, it is evident that all samples show a good cycling stability and only moderate decreases in specific capacities within 50 cycles. The best capacity and cycling performance provides PPy/PEG-LiFePO$_4$ cathode [49].

To understand the PPy and PPy/PEG coatings effect on the electrochemical performance of developed cathode materials in more detail, EIS measurements were performed with the bare LiFePO$_4$, as well as with the PPy-LiFePO$_4$ and PPy/PEG-LiFePO$_4$ composite cells (Fig. 13) [51,60]. To assure the formation of the stable solid electrolyte interface (SEI) layers on the electronic active particles the cells were cycled galvanostatically for three cycles prior the EIS measurements. So the impedance measurements were realized at entirely discharged (lithiated) conditions. Figure13 shows representative Nyquist plots of the bare LiFePO$_4$, PPy-LiFePO$_4$ and PPy/PEG-LiFePO$_4$cathodes [60]

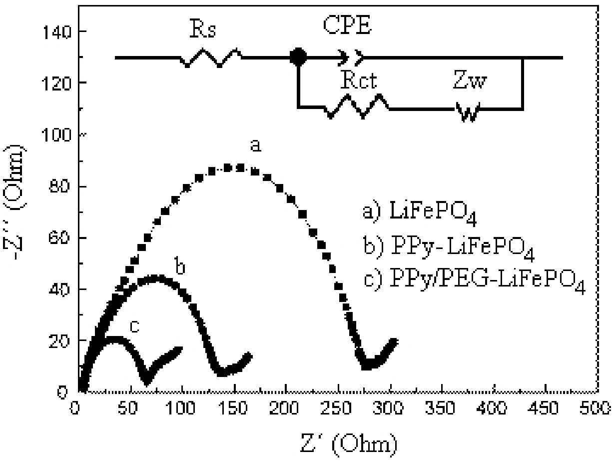

Figure 13. Nyquist plots of the bare LiFePO$_4$, PPy-LiFePO$_4$ and PPy/PEG-LiFePO$_4$ composite after three cycles and equivalent circuit used for fitting the EIS experimental data.

Impedance on the Z' at high frequency interval is associated with the resistance of the electrolyte expressed by the ohmic resistance (R_s). The semicircle appeared in the moderate frequency region represented the charge transfer resistance (R_{ct}). The sloping line at lower frequencies corresponded to the Li^+ ion diffusion in the $LiFePO_4$ particles described by the Warburg impedance (Z_w). An appropriate equivalent electrical circuit model (insert in Fig. 13) was applied for interpretation of impedance results. The double layer capacitance and passivation film capacitance was replaced with the constant phase element (CPE). There was no statistical difference between the calculated and measured values (Fig. 13) [51,60]. The parameters of the equivalent circuit were obtained from model fit for the bare $LiFePO_4$, PPy-$LiFePO_4$ and PPy/PEG-$LiFePO_4$ [51]. The lowest value of charge transfer resistance (R_{ct}) was registered for PPy/PEG-$LiFePO_4$ hybrid sample. The similar values of the electrolyte/electrode resistance (R_s) for all examined samples were obtained owing to Super P presence in the slurry which enhanced the electrical conductivity of the electrodes. The R_s value includes the ionic resistance of the electrolyte solution, the contact resistance at the current collector/active material interface and the internal resistance of the active cathode material [51]. It was found by [61] that the impedance of the cell can be mostly accounted to the cathode impedance and concretely to the charge-transfer resistance.

The highest value of exchange current density was obtained for the PPy/PEG-$LiFePO_4$ composite electrode. These results may be interpreted by the two factors: existence of polymer coating and appropriate particle size. As it was found, polymer or carbon coating improve the sample conductivity and lower the interface polarization which facilitate the Li^+ ion diffusion, and the small particle reduce the transport distance [62,63]. Porous microstructure of PPy polymer layer on the surface of $LiFePO_4$ particles facilitates the lithium ion diffusion since it render many transition crossings for Li^+ ion. Among the three examined samples, the PPy/PEG-$LiFePO_4$ cathode demonstrated the highest exchange current density and lowest resistance, indicating that the PPy/PEG coating layer could greatly improve the battery performance.

The small impedance of PPy/PEG-$LiFePO_4$ can be explained by the higher electronic conductivity resulted from the PPy/PEG network. The surface layer of PPy/PEG copolymer represents the mixed conductor of lithium ions and electrons [51].

During the charging of PPy containing electrode, two processes take place: PPy provides electrons, and anions, which compensate charge (PF_6^-) penetrated into the PPy network to sustain the charge neutrality. On the contrary, the PPy releases the anions (PF_6^-) to the electrolyte when discharging. The mentioned processes may be expressed by the following equations [64]:

$$\text{Cathode:} \quad \left[\mathrm{PPy}^0\right] - e^- + \mathrm{PF}_6^- \leftrightarrows \left[\mathrm{PPy}^+\right]\mathrm{PF}_6^- \tag{4}$$

$$\text{Anode:} \quad \mathrm{Li}^+ + e^- \leftrightarrows \mathrm{Li} \tag{5}$$

Increase in PPy content in the hybrid electrode material induces two opposite effects: reduction of the specific capacity since the practical capacity of PPy is only 72 mAh g^{-1} until the capacity of $LiFePO_4$ is 170 mAh g^{-1} and improvement of the specific capacity due to electronic conductivity enhancement resulted from PPy coating. Consequently, the value of specific capacity of PPy-$LiFePO_4$ hybrid electrode material is given by the PPy content [56].

The addition of PPy/PEG blend improves the electrical conductivity of resulting PPy/PEG-$LiFePO_4$ hybrid electrode material without the specific capacity value lowering. Therefore, the PEG additive wasapplied to improve the electronic conductivity of PPy in active cathode material. Moreover, coating of $LiFePO_4$ particles by PPy layer decreases the particle-to-particle contact resistance and due to its electronic conductivity enhances the electron transfer from the current collector. The blend PPy/PEG coating layer onto the $LiFePO_4$ particles facilitated the exchange of Li^+ ions on the surface owing to higher porosity and good salt solubility of PEG as well as the percolative transport of electrons through the polymer chain [56].

3.3 CHEMICAL COMPOSITION AND STRUCTURE OF CATHODE MATERIAL

The chemical composition and valent state of the developed PPy/PEG-$LiFePO_4$hybrid electrode materials was examined by XPS analysis.

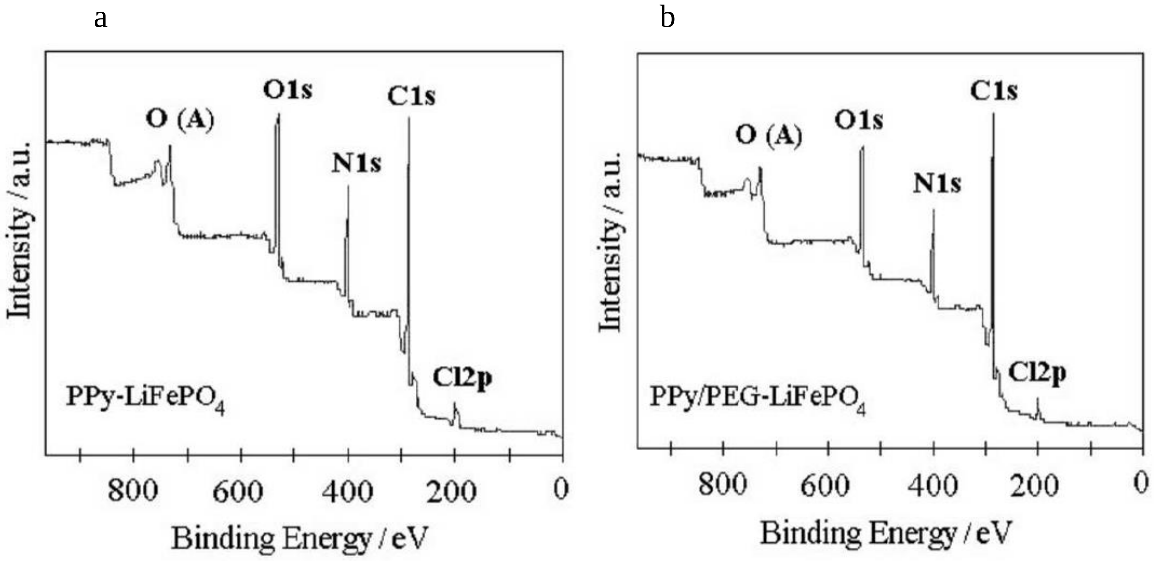

Figure 14. XPS spectra of PPy-$LiFePO_4$ (a) and PPy/PEG-$LiFePO_4$ (b) cathode material.

Results revealed differences in the surface species (Fig. 14) [51]. The binding energies (BE) of O 1s, N 1s and C 1s, were determined to be 531.2 eV, 400.0 eV and 284.4 eV respectively. There is neither Fe nor P detected by XPS, in Fig 15, the peaks at 744 eV are O KLL peaks (Auger peaks from oxygen atoms). The XPS measurement confirmed that the $LiFePO_4$ particles are completely covered with polymer coating (as described in the SEM paragraph). No peaks of Fe and P were detected on the sample surface (analysis depth is max 10 nm) [60].

The dominant peak of aliphatic carbon (284.7 eV) was observed in C 1s spectrum of both samples (Fig. 14) [51,60]. Only minor contributions from oxygenated and nitrogenated carbon can be seen on the Fig. 12 (286 and 288.4 eV). The typical peak at 291 eV is a shake-up contribution due to the π-π^* conversion in the aromatic cycle of Py monomer. Other peaks correspond to 284.7 eV - C-C / C-H, 286.4 eV - C-O / =C-N /C=N and 287.8 eV - C=O / $C=N^+$. The peak observed at 198.9 eV can be assigned to an intermediate state between that the ionic Cl^- species and the covalent –Cl species caused by an accumulation of positively charged nitrogen atoms in the polymer network [65]. The XPS results indicate that the decomposition reaction of organic solvent (EC/DMC) generated only very low amount of products such as ethers (286 – 288 eV).

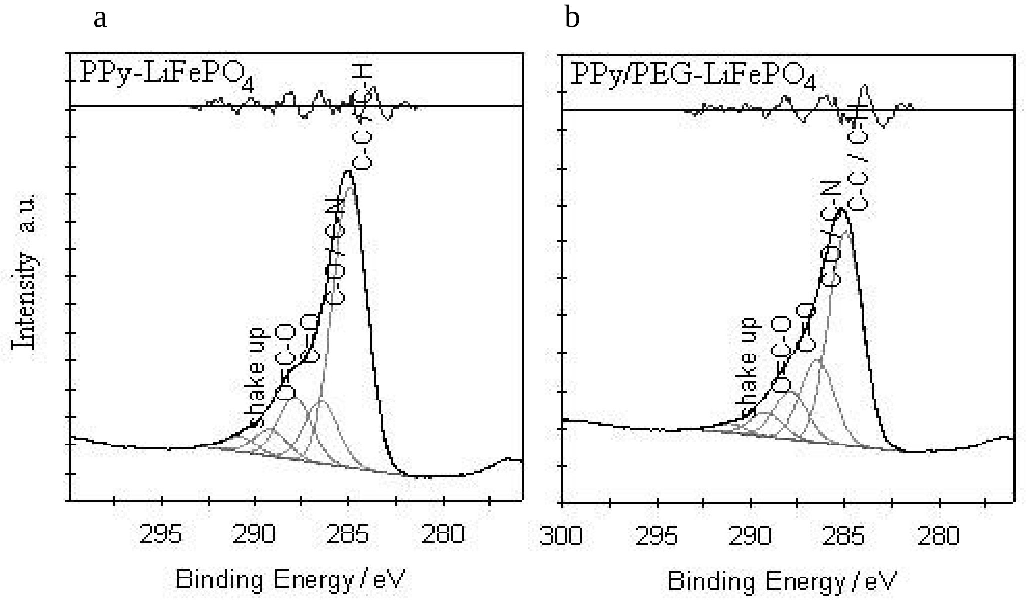

Figure 15. XPS C1s spectra for PPy-$LiFePO_4$ (a) and PPy/PEG-$LiFePO_4$ (b) cathode material.

The main difference between both samples detected from XPS spectra was the content of nitrogen and carbon. The lower content of nitrogen and higher content of carbon was detected in PPy/PEG-$LiFePO_4$ cathode in comparison with PPy-$LiFePO_4$ cathode due to the polymer coatings. The N1s response registered in spectra at 400 eV was resolved using fitting into two peaks at 400 eV and 402 eV, which can be attributed to the N–H and N–C bonds [66]. The O1s peaks recorded at 532.2 eV evidenced the presence of adsorbed oxygen in the samples coming from environment. Lack of peaks at 390 eV and 406 eV in the spectra confirm the absence of bonds between O and C or N, which proves that the polymer films are not in oxidized state [51,60].

The surface composition and structure of developed PPy/PEG-$LiFePO_4$ cathode material was evaluated by means of ToFSIMS analysis. To evaluate the effect of polymeric coating layer on the structure and stability of cathode materials the both active hybrid electrode materials (PPy-$LiFePO_4$ and PPy/PEG-$LiFePO_4$) and both polymers (PPy and PPy/PEG with PVDF) were analyzed. Overlay of the ToFSIMS spectra of PPy + PVDF and PPy/PEG + PVDF is shown in Fig. 16 [56].

Only a few intensive cluster peaks in mass range below 150 m/z were observed in the spectrum of single PPy. The polymeric behaviour with the repetition of mass unit 102 m/z beginning from the 247 m/z up to 3205 m/z dominates in the spectrum of PPy/PEG co-polymer. This repeating mass unit 102 m/z belongs to fragment $[C_5OH_{12}N]^+$ created from the one Py ring and fraction of PEG molecule as given by Eq. (6):

$$\mathrm{H} + \mathrm{O} - (\mathrm{CH_2})_5 - \mathrm{NH} +^{+} \tag{6}$$

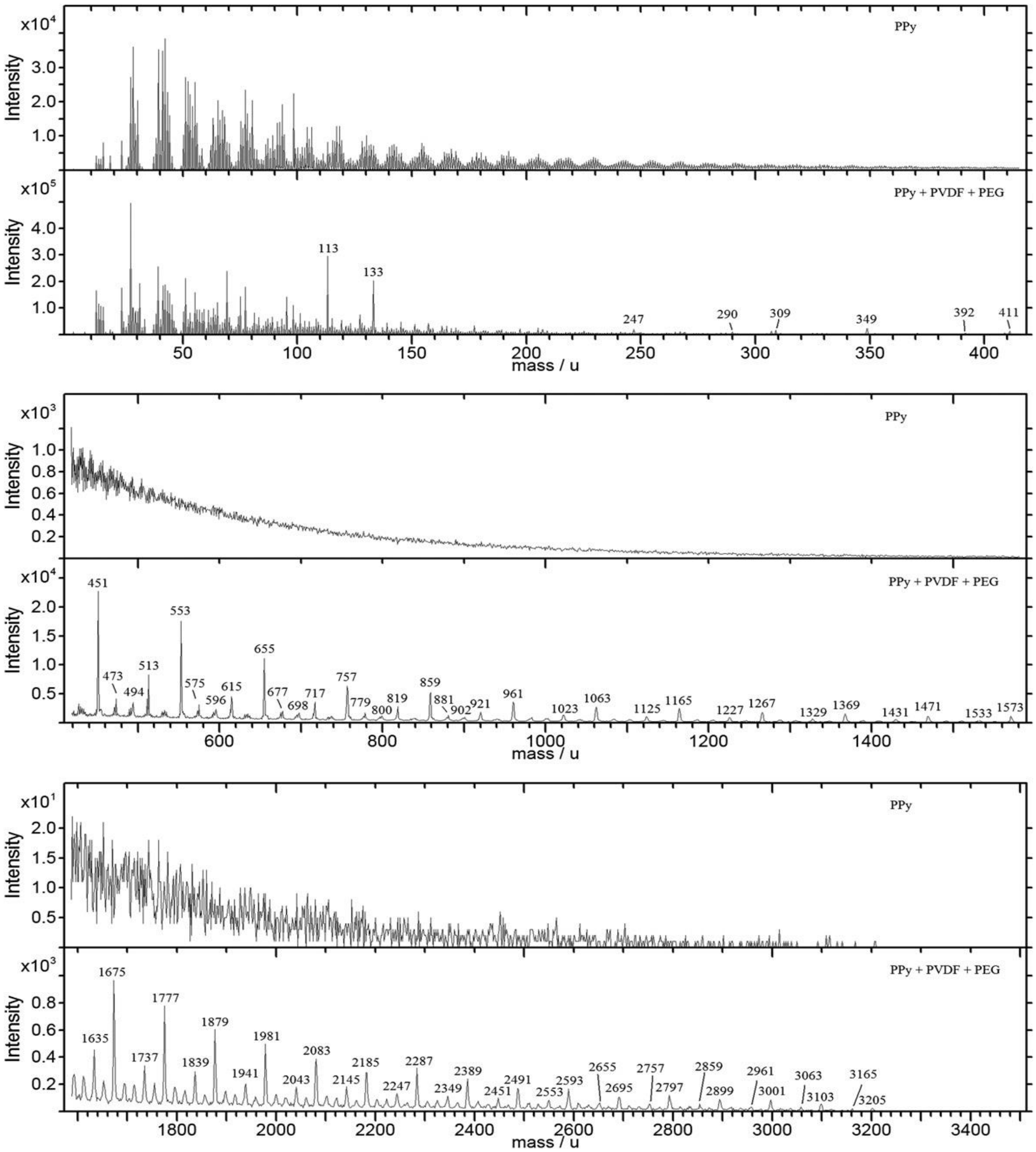

Figure 16. Overlay of positive ToF SIMS mass spectra of PPy + PVDF and PPy/PEG + PVDF.

The above mentioned fragment 247 m/z is besides the same building units as the fragment 102 m/z composed of two opened and saturated Py rings and the PEG molecule fragments on both ends:

$$H \left[O - (CH_2)_5 - NH \right]_2^+ - O - (CH_2)_2 \qquad (7)$$

Another three peaks with m/z 62, 43 and 22 can be found inthis repeating unit (Eq. (7)). The ion 62 m/z belongs to fragment 102 m/z reduced by CH_2CN and 43 m/z to form the $[PEG{-}H]^+$ monomer. The repetitive element with 22 m/z suits to $[H_3F]^+$which came from the PVDF likewise the high fragments 133 m/z corresponding to $[C_3F_5H_2]^+$ and 113 m/z which originated from fragment 133 m/z withdrawing one molecule of HF. Addition of PEG to the PPy establishes more stable polymeric structure required in efficient cathode materials for LIBs [56].

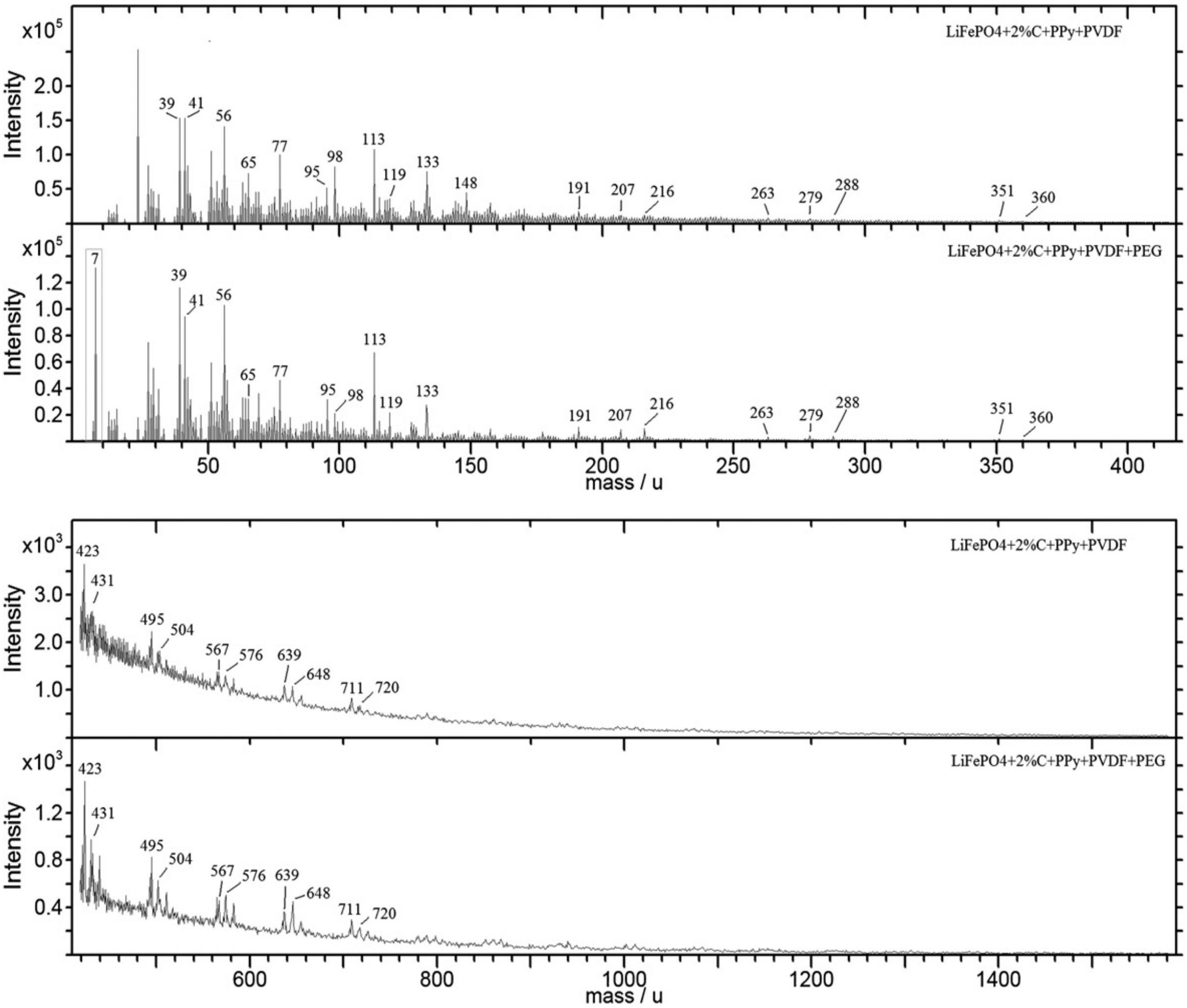

Figure 17.Overlay of the positive ToFSIMS spectra of $LiFePO_4$+ 2%C + PPy+ PVDF with and without PEG.

Only a few differences, particularly in the mass range up to 150 m/z, were detected from the positive ToFSIMS spectra of cathode materials prepared by mixing of $LiFePO_4$ particles with PPy + PVDF without and with PEG depicted in Fig. 17 [56].

The more intensive fragments were observed in spectra of cathode material without PEG. Only exception represented the Li^+ ion, which showed high intensity in the spectrum of cathode material with PEG additive but it absented in the sample without PEG. This contrast confirmed the good conductivity of Li^+ ions in the PPy/PEG co-polymer. The stable polymeric structure with the mass unit 72 m/z corresponding to FeO fragment repetitive in the range from 207 m/z to cca. 1000 m/z can be observed in both spectra. The other characteristic SIMS fragments of PPy/PEG-$LiFePO_4$material mixed with + PVDF were predominantly consisting of two PPy rings, one H_2 molecule, Fe or FeO and in some cases also LiH_2 [56].

Results of the ToF SIMS analyze proved the assumption that PEG addition facilitates the Li^+ ion solubility in the cathode material and enhances its migration through the PPy/PEG layer (Fig. 15). The distribution of the positive lithium ions on the surface of cathode materials with (a) and without PEG (b) admixture can be observed from the ToF SIMS images showing on Fig. 18 [56]. Addition of PEG sustains the PPy chain structure resulting in more stable and coherent cathode material with homogeneous distribution of Li^+ ions as confirmed by Fig. 18a.

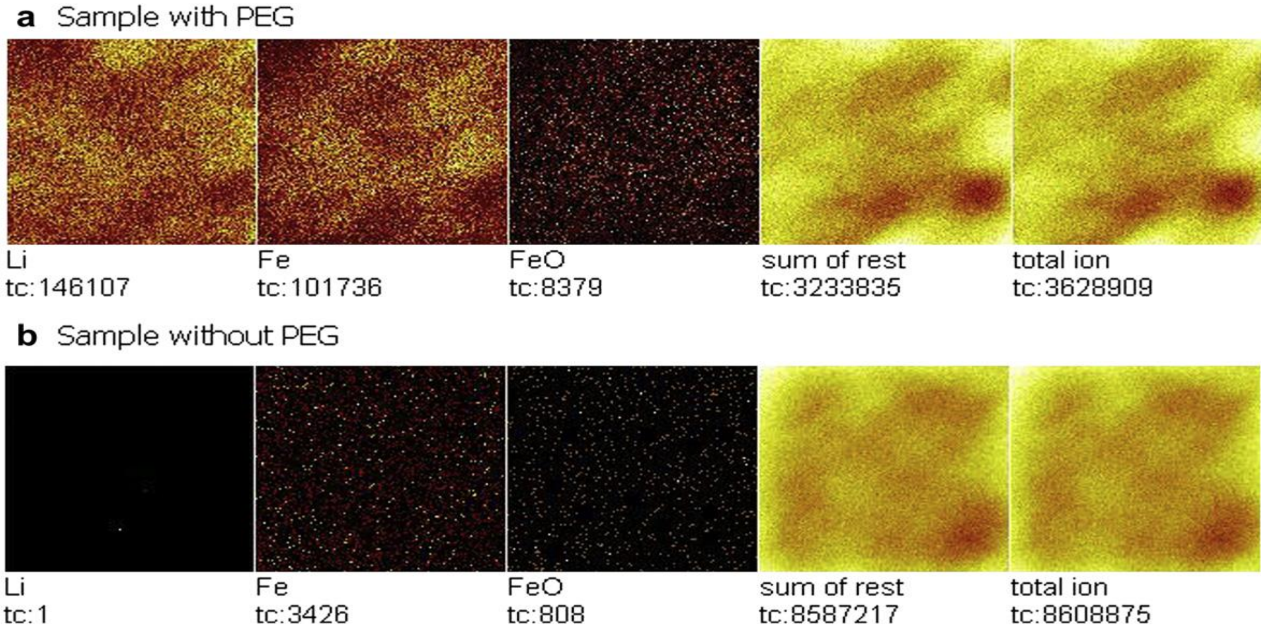

Figure 18. ToF SIMS images of the positive ions distribution on the surface of cathode materials with (a) and without PEG additive(b).

Diffusion of Li^+ ion from the surface deeper into the cathode material probably caused that the primary ion gun cannot to reach it and thus it not appeared in the mass spectrum of the cathode material without PEG (Fig. 18b) [56].

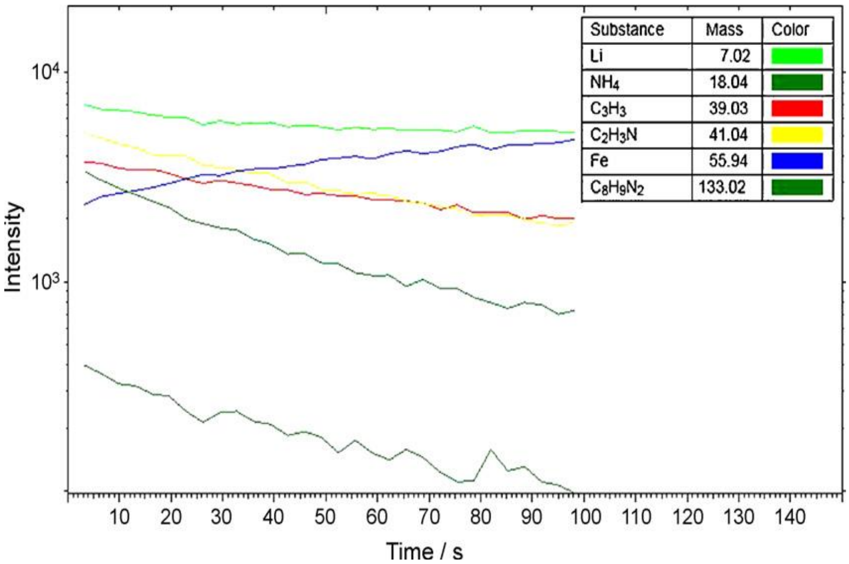

Figure 19. Depth profile of PPy/PEG–$LiFePO_4$ material.

The characteristic ToF SIMS depth profile of PPy/PEG–$LiFePO_4$ cathode material depicted in Fig. 19 exhibits the distribution of the PPy/PEG coating on the surface of $LiFePO_4$ particles [47,56]. The six characteristic fragments: Li^+, NH_4^+, $C_3H_3^+$, $C_2H_3N^+$, Fe^+ and $C_8H_9N_2^+$ were selected to monitor the coating layer – particle surface interface. While the Fe^+ ion represents the inner species originated from $LiFePO_4$ particle, remaining fragments represent the outer species coming from PPy/PEG coating layer. The high intensity and nearly constant profile of Li^+ curve means that the distribution of Li differs only moderately from the surface to the depth [47,56].This behaviour approved diffusion of Li^+ ions from the $LiFePO_4$ particle to the PPy/PEG layer. The increase in the intensity of Fe^+ ion and decrease in the intensity of NH_4^+ fragment resulted from PPy ring was detected with increasing depth. The intensity curve of Fe^+ ion crossed the intensity curve of NH_4^+ at about 10 s. Considering the average rate of sputtering beam about 10 nm s^{-1}, it corresponds to the thickness of PPy approximately 100 nm.

The ToF SIMS and XPS analyses accredited the presence of uniform PPy/PEG coating layer on the $LiFePO_4$ particle surface and confirmed that the PPy/PEG–$LiFePO_4$ is a unique and promising hybrid cathode material for rechargeable LIBs [47,56].

4 CONCLUSIONS

The effect of PPy/PEG polymer layer on the structural characteristics as well as on the electrochemical performance of $LiFePO_4$ based cathode material for high-performance LIBs was highlighted in this short version of habilitation thesis.

The PPy/PEG-modified $LiFePO_4$ cathode material may be produced by the oxidative polymerization in an aqueous suspension, which constitutes the very simple synthesis way of the stabile polymers.

PPy coating on the $LiFePO_4$ particle surface increases the specific surface area, porosity and conductivity of the as-prepared cathode material.

Addition of PEG enhances the stability and conductivity of polymeric coating layer. The PPy/PEG co-polymer is characterized by more stable polymeric structure than the bare PPy. Moreover, introduction of PEG in cathode material facilitates the solubility and insertion/extraction of the Li^+ ion in the matrix.

Modification of $LiFePO_4$ cathode material with the PPy/PEG coating improves the charge transfer rates, the charging/discharging characteristics, and the electrode activity. PPy/PEG coating facilitates insertion of both electrons and lithium ions in the three-dimensional structure of $LiFePO_4$ based cathode material. Results of cyclic voltammetry and AC impedance measurements approved the positive effect of PPy/PEG blend polymer on the improvement of the charge transfer reaction kinetics which can be interpreted by the good mixed electronic and ionic conductivity of the PPy/PEG coating layer. Results of charge/discharge measurements demonstrated the capacity increase due to addition of PEG. The considerable higher current density and enhanced efficiency was achieved for PPy/PEG–$LiFePO_4$ cathodes as compared withPPy-$LiFePO_4$ and bare $LiFePO_4$ cathodes.

Application of PPy/PEG coating introduces the innovative impact to the development of promising $LiFePO_4$ based positive electrode material for LIBs, granting the high specific charge, stable and reversible capacity and good reversibility even under high rate cycles.

5 REFERENCES

[1] M. R. Palacin, Chem. Soc. Rev., 38 (2009) 2565.
[2] Y. Nishi, Chem. Rec., 1(2001) 406.
[3] D. Guerard, A. Herold, Carbon, 13 (1975) 337.
[4] M. S. Whittingham, Prog. Solid State Chem., 12 (1978) 41.
[5] M. Armand, J. M. Tarascon, Nature, 451 (2008) 652.
[6] M. S. Whittingham, Chem. Rev., 104 (2004) 4271.
[7] B. L. Ellis, K. T. Lee, L. F. Nazar, Chem. Mater., 22 (2010) 691.
[8]P. G. Bruce, S. A. Freunberger, L. J. Hardwick, J. M. Tarascon, Nat. Mater., 11(2012) 19.
[9] X. L. Ji, L. F. Nazar, J. Mater. Chem., 20 (2010) 9821.
[10] A. Manthiram, Y. Fu, Y.-S. Su, Acc. Chem. Res., 46 (2013) 1125.
[11]Mineral commodity summaries 2013, U.S. Geological Survey, Reston, Virginia, 2013.
[12] A. Volta, Phil. Mag., 7 (1800) 31.
[13] J.-M.Tarascon and M. Armand, Nature, 414 (2001) 359.
[14] H. Ikeda, T. Saito and H. Tamura, in Proc. Manganese Dioxide Symp., Vol. 1
(Eds A. Kozawa and R.H.Brodd), IC Sample Office, Cleveland, OH (1975).
[15] M. S. Whittingham, US Patent 4009052.
[16] M. S. Whittingham, A. J. Jacobson, Intercalation Chemistry, Academic press, New York (1982).
[17] K. Mizushima, P. C. Jones, P. J. Wiesman, J. B. Goodenough, Mater. Res. Bull., 15 (1980) 783.
[18] J. B. Goodenough, K. Mizushima, T. Takeda, J. Appl. Phys., 19 (1985) 305.
[19] M. M. Thackeray, W. I. F. David, P. G. Bruce, J. B. Goodenough, Mat. Res. Bull., 18 (1983) 461.
[20] S. Megahed, B. Scrosati, Interface, 4 (4) (1995) 34.
[21] Z. Takehare, K. Kanamura, Electrochim. Acta, 38 (1993) 1169.
[22] M. L. B. Rao, U.S. Pat., 3 413 154 (1968).
[23] D. Nole, V. Moss, U.S. Pat., 3 532 543(1970).
[24] A. J. Gmitter, F. Badway, S. Rangan, R. A. Bartynski, A. Halajko, N. Pereira, G. G. Amatucci, J. Mater. Chem**.,** 20 (2010) 4149.
[25] J. D. Schuster, Morphology Control of Ordered Mesoporous Carbons for High Capacity Lithium Sulfur Batteries, dissertation thesis (2011), München
[26] http://www.mpoweruk.com/lithiumS.htm, available January 2014.
[27]M. Winter, J. O. Besenhard, M. E. Spahr, P. Novák, Advanced Materials, 10 (1998) 725.
[28] N. Daumas and A. Hérold, Bull. Soc. Chim.,5 (1971) 1598.
[29] J. R. Dahn, Phys. Rev. B, 44 (1991) 9170.
[30] A. K. Padhi, K.S. Nanjundaswamy, J. B. Goodenough, J. Electrochem. Soc., 144 (1997) 1108.
[31] A.S. Andersson, J.O. Thomas, J. Power Sources, 97 (2001) 498.
[32] N. Ravet, J. B. Goodenough, S. Besner, M. Simoneau, P. Hovington, M. Armand, Abstract #127, 196th Meeting ofthe Electrochemical Society, Hawaii (1999).
[33] H. Huang, S.-C. Yin, L. F. Nazar, Electrochem. Solid-State Lett., 4 (2001) A170.
[34] R. Dominko, M. Bele, M. Gabarscek, M. Remskar, D. Hanzel, S. Pejovnik, J. Jannik, J. Electrochem. Soc., 152 (2005) A607.
[35] A. Yamada, S. C. Chung, K. Hinokuma, J. Electrochem. Soc., 148 (2001) A224.
[36] S. Yang, P.Y.Zavalij, M.S.Whittingham, Electrochem. Comm., 3 (2001) 505.
[37] P. P. Prosini, M. Carewska, S. Scaccia, P. Wisniewski, S. Passerini, M. Pasquali, J. Electrochem. Soc., 149 (2002) A886.
[38] A. S. Andersson, J. O. Thomas, B. Kalska, L. Häggström, Electrochem. Solid-State Lett., 3 (2000) 66.

[39] D. Singh, W.-S. Kim, V. Craciun, H. Hofmann, R. K. Singh, Appl. Surf. Sci., 197/198 (2002)516.
[40] D. Linden, Handbook of Batteries, 2nd Edition, McGraw Hill, NJ, pp. 36.1–36.14.
[41] Y. Gao, J. R. Dahn, J. Electrochem. Soc., 143 (1996) 100.
[42] A. Rougier, K. A. Striebel, S. J. Wen, T. J. Richardson, R. P. Reade, E. J. Cairns, Appl. Surf. Sci., 135 (1998) 107.
[43] H. Yamin, A. Gorenshtein, J. Penciner, E. Peled, J. Electrochem. Soc., 135 (1998) 1045.
[44] H. Yamin, E. Peled, J. Power Sources, 9(1983) 281.
[45] H. Yamin, J. Penciner, A. Gorenshtein, M. Elam, E. Peled, J. Power Sources, 14 (1985) 129.
[46] Y. Jung, Int. J. Electrochem. Sci., 3 (2008) 566.
[47] A. Fedorková, R. Oriňáková, A. Oriňák, I. Talian, A. Heile, H. D.Wiemhöfer, D. Kaniansky, H. F. Arlinghaus,J. Power Sources, 195 (2010) 3907.
[48] Y. H. Huang, K. S. Park, J. B. Goodenough, J. Electrochem. Soc., 153 (2006) A2282–A2286.
[49] A. Fedorková, A. Nacher-Alejos, P. Gómez-Romero, R. Oriňáková, D. Kaniansky, Electrochim. Acta, 55 (2010) 943–947.
[50] A. Fedorková, H. D. Wiemhöfer, R. Oriňáková, A. Oriňák, D. Kaniansky, Solid State Scie., 12 (2010) 924.
[51] A. Fedorková, R. Oriňáková, A. Oriňák, M. Kupková, H. D.Wiemhöfer, J. N. Audinot, J. Guillot, Solid State Scie., 14 (2012) 1238.
[52] N. Toshima, O. Ihata, Synthetic Metals, 79 (1996)165.
[53] M. R. Nabid, A. A. Entenzami, European Polymer Journal, 39 (2003) 1169.
[54] H. C. Kang, K. E. Geckeler, Polymer, 41 (2000) 6931.
[55] A. Fedorková, H. D. Wiemhöfer, R. Oriňáková, A. Oriňák, M. C. Stan, M. Winter, D. Kaniansky, A. Nacher Alejos, J. Solid State Electrochem., 13 (2009) 1867.
[56] A. Fedorková, R. Oriňáková, A. Oriňák, A. Heile, H. D. Wiemhöfer, H. F. Arlinghaus, Solid State Scie., 13 (2011) 824.
[57] F. Croce, A. D´Epifanio, J. Hassoun, A. Deptula, T. Olczac, B. Scrosati, Electrochem. Solid-State Lett., 5 (2002) A47.
[58] M. Takahashi, S. Tobishima, K. Takei, Y. Sakuri, Solid State Ionics, 148 (2002) 283.
[59] A. Fedorková, R. Oriňáková, A. Oriňák, H. D. Wiemhöfer, D. Kaniansky, M. Winter, J. Solid State Electrochem., 14 (2010) 2173.
[60] A. Fedorková, R. Oriňáková, A. Oriňák, H. D. Wiemhöfer, J. N. Audinot, J. Guillot, ECS Transactions, 40 (2012)107.
[61] C. H. Chen, J. Liu, K. Amine, J. Power Sources, 96 (2001) 321.
[62] S. J. Kwon, C. W. Kim, W. T. Jeong, K. S. Lee, J. Power Sources, 137 (2004) 93.
[63] J. L. Li, C. Daniel, D. Wood, J. Power Sources, 196 (2011) 2452.
[64]G. X. Wang, L. Yang, Y. Chen, J. Z. Wang, S. Bewlay, H. K. Liu, Electrochim. Acta, 50 (2005) 4649.
[65] J. F. Marco, J. R. Gancedo, H. Nguyen Cong, M. del Canto, J. L. Gautier, Solid State Ionics, 177 (2006) 1381.
[66] S. K. Swathi, T. Jeevananda, P. C. Ramamurthy, Organic Electronics, 11 (2010) 1489

ABSTRACT

This thesis represents a broad overview dealing with preparation and characterization of new cathode materials for Li-ion batteries based on $LiFePO_4$. Fundamental conclusions were published by the applicant in 12 peer-reviewed papers from 2009 to 2013 and all of them are a part of the thesis. The theoretical part of the thesis is focused on problems of cathode materials based on intercalation and conversion reaction. The first part of the research itself is devoted to the complete characterization of $LiFePO_4$ cathode material modified by different techniques and additives. Considerable efforts have been made to enhance the electronic conductivity and Li^+ diffusion in the cathode materials. To fabricate composite cathodes comprising oxides and electrochemically active conducting polymers is also a potential approach to improve the electronic conductivity and Li^+ diffusion. Polypyrrole (PPy (with theoretical capacity 70 mAh/g)) is a typical conducting polymer, which also acts as a host material for Li^+ion insertion/extraction. In this work, polyethyleneglycole (PEG) is introduced into polypyrrole (PPy) film coated on $LiFePO_4$ powder particles to promote the properties of cathode material for lithium-ion batteries. The enhancement of the electrochemical activity by the substitution of carbon with electrochemically active polymer is investigated. Cyclic voltammetry (CV), electrochemical impedance spectroscopy (EIS) and galvanostatic charge/discharge measurements were employed to characterize the electrochemical properties of PPy/PEG-$LiFePO_4$ material. The electrochemical performance of PPy-$LiFePO_4$ electrodes was greatly improved by introduction of PEG into the PPy films. Charge/discharge measurements confirmed the increase in capacity when applying PEG in PPy. Last part of applicant research is focused on new type of cathode material with conversion reaction – sulfur. Combination of conversion material (sulfur) with intercalation material ($LiFePO_4$) blended with PPy and PEG will be the next step in developing of new cathode material with better performance, cyclability and high capacity.

ABSTRAKT

Táto práca predstavuje prehľad zaoberajúci sa prípravou a charakterizáciou nových katódových materiálov pre Li-ion batérie na báze $LiFePO_4$. Hlavné výsledky boli publikované v 12 recenzovaných článkoch v rokoch 2009-2013 a všetky z nich sú súčasťou práce. Prvá časť výskumu je venovaná kompletnej charakterizácií $LiFePO_4$ katódového materiálu modifikovaného rôznymi prísadami a technikami. Hlavným cieľom bolo zvýšiť elektrónovú a iónovú vodivosť katódových materiálov, ktoré sú bežne nevodivé, alebo majú len nízku vodivosť. Použitím vodivého polyméru polypyrolu (PPy) sa zvýšila vodivosť a zároveň aj kapacita výsledného kompozitného materiálu. Polypyrol totiž sám pracuje ako katódový materiál s teoretickou kapacitou okolo 70 mAh/g. Taktiež sa zlepšila difúzia Li^+ do štruktúry katódového materiálu, vďaka použitiu nevodivého polyméru polyetylénglykolu (PEG). Vlastnosti týchto materiálov sa skúmali pomocou cyklickej voltampérometrie (CV), elektrochemickej impedančnej spektroskopie (EIS) a pomocou galvanostatického nabíjania/vybíjania. Pridaním kompozitného polyméru PPy/PEG sa zvýšila cyklovateľnosť, kapacita a stabilita katódového materiálu. Ďalším krokom bude preskúmať vlastnosti katódového materiálu v kombinácií interkalačného materiálu ($LiFePO_4$) a konverzného materiálu (síry). Nové materiály ako síra či kremík majú veľký potenciál nahradiť dnešné materiály pracujúce na princípe interkalácie a zvýšiť tým kapacitu batérií aj 10-násobne.